American Mineralogist, Volume 70, pages 237–248, 1985

Equilibria in the system MgO–SiO_2–H_2O: a thermodynamic analysis

HOWARD W. DAY

Department of Geology
University of California, Davis, California 95616

J. V. CHERNOSKY

Department of Geological Sciences
University of Maine, Orono, Maine 04469

AND H. J. KUMIN

School of Industrial Engineering
University of Oklahoma, Norman, Oklahoma 73019

Abstract

Thermodynamic analysis of experimentally determined reactions among H_2O and the nine minerals: antigorite, anthophyllite, brucite, chrysotile, enstatite, forsterite, periclase, quartz, and talc, shows that the available calorimetrically determined enthalpies and entropies are not compatible with the hydrothermal experiments. Major discrepancies appear to exist for the enthalpies of formation of talc and enstatite and for the entropy of anthophyllite. The experimental data, molar volumes and heat capacities are internally consistent, however, and permit only one topology of phase diagram for Mg-anthophyllite, that first proposed by Greenwood (1963). Our "best" set of thermodynamic parameters, internally consistent with these data, includes values for the enthalpy of formation from the elements (298 K, 1 bar) of antigorite and anthophyllite: −71435 kJ and −12073 kJ respectively.

Introduction

Mineral equilibria in the system MgO–SiO_2–H_2O represent a model for metamorphism of calcium-poor ultramafic rocks and, if thoroughly understood, could form reliable starting points for further thermodynamic or experimental exploration of equilibria that approximate natural reactions. Unfortunately, no consensus has yet emerged concerning either the basic topology of the phase diagram or the thermodynamic properties of phases in this system.

Greenwood (1963) and Hemley et al. (1977) determined equilibria among the phases anthophyllite (A), enstatite (E), forsterite (F), quartz (Q), talc (T) and H_2O (W) and proposed phase diagrams that differed largely in the calculated or assumed location of the water-conservative reaction T + E = A (see Fig. 1). Delaney and Helgeson (1978) calculated a phase diagram similar to the one proposed by Greenwood (1963) except that the invariant points were at much lower pressure. Day and Halbach (1979) used experimental data on four reactions reported by Chernosky (1976) and Chernosky and Knapp (1977) to derive thermodynamic parameters for eleven reactions among these six phases. They showed that calculated phase diagrams could have any of the topologies previously proposed as well as several others that had not been considered. All such calculated diagrams were consistent with the experiments and with the known heat capacities and volumes of the participating phases but major discrepancies existed between the calculated enthalpy or entropy of talc and that determined calorimetrically.

Experimental and calorimetric data have appeared since 1979 that warrant a new attempt to evaluate the stability field of anthophyllite and to extend the thermodynamic evaluation to equilibria involving antigorite (An), brucite (B), chrysotile (C), and periclase (P).

The purpose of this paper is to analyze these new experimental and calorimetric data in the system MgO–SiO_2–H_2O. We hope to show that the experiments, heat capacities and molar volumes of the phases are internally consistent and that only one thermodynamically consistent phase diagram topology is permitted by these data. The experimental data appear to be incompatible with existing calorimetrically derived enthalpies and entropies of some of the individual phases. Possible sources of these discrepancies are the measured enthalpies of talc and enstatite and the heat capacity function or entropy of anthophyllite.

The compositions of phases are illustrated in Figure 2 and some of their properties are summarized in Table 1. The equilibria with which we are concerned are listed in Table 2 together with the equations that describe the linear dependence of the reactions.

0003–004X/85/0304–0237$02.00

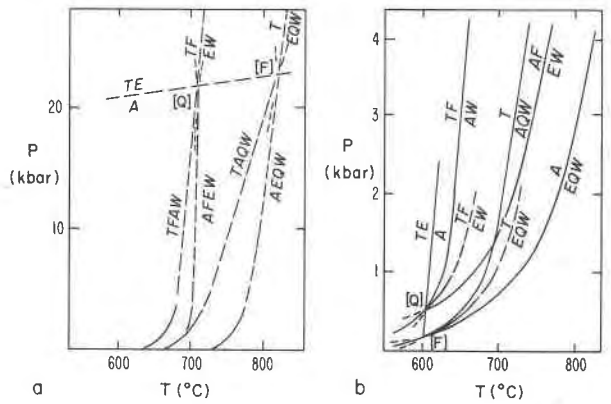

Fig. 1. Two topologies proposed for equilibria among anthophyllite, enstatite, forsterite, quartz, talc and water by (a) Greenwood, 1963 and (b) Hemley et al. (1977). Note that reactions TFEW and TEQW are stable only at high pressure in (a) and at low temperature in (b). Note differences in scale in the two diagrams.

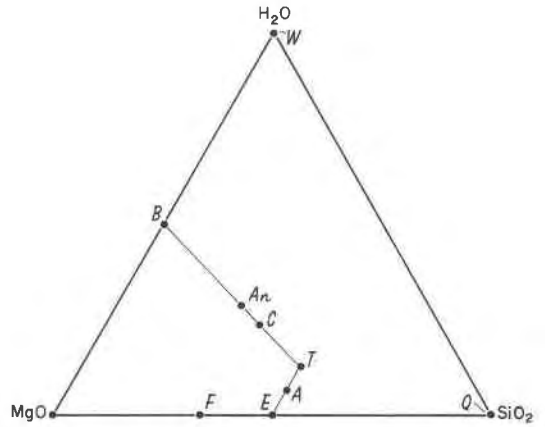

Fig. 2. Molar compositions of minerals in the system MgO–SiO_2–H_2O.

Methods of thermodynamic analysis

Our approach is based on the thermodynamic analysis of phase equilibria discussed by Zen (1969), Chatterjee (1970, 1977), and Fisher and Zen (1971). We have evaluated the permissible thermodynamic solutions to the phase equilibria using the linear programming methods first described by Gordon (1973), and further developed by Day and Halbach (1979) and Day and Kumin (1980). The equilibrium condition for a dehydration reaction may be written (notation is summarized in Table 3):

$$\Delta G_r(T,P) = \Delta H^\circ_{fs}(298,1) - T\Delta S^\circ_{fs}(298,1) + G'(T,P) \qquad (1)$$
$$= 0$$

All terms involving the fluid phase and all terms describing the deviation of the solid phases from 298 K, 1 bar are included in the right-hand term in equation (1):

$$G'(T,P) = \int_{298}^{T} \Delta C_{Pfs}\, dT - T \int_{298}^{T} \Delta C_{Pfs}/T\, dT + \Delta V_s(P-1) + N_w G^*_w(T,P).$$

This description of the equilibrium condition ignores the small

Table 1. Composition and properties of phases in the system magnesia–silica–water

Phase		Formula Unit	Volume	Heat Capacity Coefficients[6]				
			(cm^3)	A	B	C	D	E
Antigorite	(An)	$Mg_{48}Si_{34}O_{85}(OH)_{62}$	1749.13[1]	5615.83	1554.45	-1554.75	0	0
Anthophyllite	(A)	$Mg_7Si_8O_{22}(OH)_2$	264.46[2]	774.018	270.025	-191.912	0	0
Brucite	(B)	$Mg(OH)_2$	24.63[3]	104.375	13.334	-28.567	0	0
Chrysotile	(C)	$Mg_3Si_2O_5(OH)_4$	108.5[3]	346.98	95.019	-95.759	0	0
Enstatite	(E)	$MgSiO_3$	31.29[4]	103.063	27.432	-26.552	0	0
Forsterite	(F)	Mg_2SiO_4	43.79[3]	227.98	3.4139	-8.9397	0	-1744.6
Periclase	(P)	MgO	11.248[3]	65.211	-1.2699	-4.6185	0	-387.24
α Quartz	(Q)	SiO_2	22.688[3]	46.945	34.309	-11.297	0	0
β Quartz					60.291	8.117	0	0
Talc	(T)	$Mg_3Si_4O_{10}(OH)_2$	136.26[5]	403.145	118.040	-103.308	0	0

1 Evans et al. (1976)
2 Greenwood (1963)
3 Robie, Hemingway and Fisher (1978)
4 Stephensen, Sclar, and Smith (1966)
5 Stemple and Brindley (1960)
6 $Cp = A + BT\,(10^{-3}) + CT^{-2}(10^5) + DT^2(10^{-6}) + ET^{-1/2}$ (J/K)
The heat capacity functions of forsterite and periclase were taken from Robie, Hemingway, and Fisher (1978). The remainder are discussed in the text.

Table 2. Reactions and equations of linear dependence in the system magnesia–silica–water

		Reaction	Reference	Linear Dependence
R1.	(TEQW)	T = 3E + Q + W	1	R5 + 3R4 - 7R1 = 0
R2.	(TFEW)	T + F = 5E + W	1	R4 + R7 - R1 = 0
R3.	(AFEW)	A + F = 9E + W	1	R2 - R3 - R7 = 0
R4.	(AEQW)	A = 7E + Q + W	1	9R2 - R6 - 5R3 = 0
R5.	(TAQW)	7T = 3A + 4Q + 4W	1	
R6.	(TFAW)	9T + 4F = 5A + 4W	1	
R7.	(TEA)	T + 4E = A	1	
R8.	(CFTW)	5C = 6F + T + 9W	2	
R9.	(CBFW)	C + B = 2F + 3W	3	
R10.	(AnFTW)	An = 18F + 4T + 27W	4	
R11.	(BPW)	B = P + W	5,6	

[1]Chernosky et al. (1984)
[2]Chernosky (1982)
[3]Johannes (1968)
[4]Evans et al. (1976)
[5]Schramke et al. (1982)
[6]Barnes and Ernst (1963)

effects of isothermal compressibility and thermal expansion on the molar volumes of the solid phases but is otherwise exact. Thermal expansion and compressibility are unknown for many phases and it is not clear whether estimating these properties improves the thermodynamic analysis or whether it introduces more uncertainty than it removes. Consequently, we have chosen not to express the molar volumes of the solids as functions of pressure and temperature.

Most hydrothermal experiments define limits on the location of an equilibrium curve rather than estimates of the true equilibrium temperature or pressure. If the products of a reaction grow at the expense of the reactants then

$$\Delta G_r(T,P) < 0 \tag{2}$$

or

$$\Delta H^\circ_{fs}(298,1) < T\Delta S^\circ_{fs}(298,1) - G'(T,P)$$

Likewise, if the reactants grow at the expense of the products:

$$\Delta G_r(T,P) > 0 \tag{3}$$

or

$$\Delta H^\circ_{fs}(298,1) > T\Delta S^\circ_{fs}(298,1) - G'(T,P)$$

Linear programming analysis requires, however, that expressions (2) and (3) be written as $\leq$ or $\geq$ inequalities implying that the equilibrium curve might actually pass through a pressure-temperature coordinate at which significant reaction was observed. Clearly, the $\leq$ or $\geq$ inequalities would be a thermodynamically incorrect description of the experiments, but the discrepancy is of no practical consequence because the observed temperature brackets could be narrowed by an arbitrary fraction of one degree Celsius so that these inequalities would be formally correct. After substituting $\leq$ or $\geq$ inequalities, expressions such as (2) or (3) define a straight line on a graph of ΔH°_{fs} versus ΔS°_{fs} having a slope equal to the temperature of the experiment. Combinations of enthalpy and entropy violating the experiment lie on one side of the line while combinations satisfying these inequalities lie on the other side and on the line itself. A set of such experimentally derived constraints may define a closed region containing all solutions consistent with the limiting experiments, molar volumes, heat capacities and properties of H_2O (e.g., Fig. 4., Day and Halbach (1979) or Fig. 4, this paper).

It is clear from expressions (2) and (3) that the enthalpy and entropy of the solids in a reaction may be constrained using hydrothermal experiments provided that heat capacities and molar volumes are available for the participating solids and that the thermodynamic properties of H_2O are known. We have calculated values of $G^*_w(T,P)$ (Table 3) using the subroutines published by Holloway et al. (1971), which are based on the properties of H_2O determined by Burnham et al. (1969). Molar volumes are listed in Table 1 together with heat capacity functions for the minerals considered.

Molar volume data

The molar volumes we have used are taken from the literature (Table 1) for both natural and synthetic phases. The unit cell volumes of phase synthesized for this study (Chernosky et al., 1985) are within the range of values reported in the literature and comparable to those used in the thermodynamic calculations. We chose to accept the values already in the literature because our refinements were very sensitive to the method of refinement used and were made on phases synthesized during runs of several days. Thus, we cannot rule out the possibility that the molar volumes would continue to change slightly in experiments that last up to almost 5000 hours.

Heat capacity data

We used the heat capacities that are listed in Table 1 as extended Maier-Kelley functions of temperature. We prefer to avoid using a T^2 term in the function because such terms prohibit theoretically reasonable extrapolations outside the temperature range for which experimental data are available (cf. Day and Halbach, 1979, p. 814). Heat capacity functions for the elements were taken directly from Robie et al. (1978) despite the presence of T^2 terms because no extrapolations were required for these data.

For periclase and forsterite, we used the heat capacity functions reported by Robie et al. (1978). Robie, Hemingway, and Takei (1982) reported a slightly revised heat capacity function for forsterite but we retained the earlier function because it reproduces the heat content data of Orr (1953) somewhat better for temperatures up to 725°C.

Heat capacities for anthophyllite, enstatite, and talc are based

Table 3. Thermodynamic notation

T,P,V	Temperature (K), Pressure (bars), Volume (cm^3)
H°_f	Standard state enthalpy of formation from the elements (J/gfw) (298 K, 1 bar)
S°_f	Standard state entropy of formation from the elements (J/K-gfw) (298 K, 1 bar)
S°	Third law entropy (J/K-gfw) (298 K, 1 bar)
C_{pf}	Heat capacity of formation from the elements (J/K-gfw)
G_f	Gibbs energy of formation from the elements (J/gfw)
G^*_w	$G_{f,H_2O}(T,1) + G_{H_2O}(T,P) - G_{H_2O}(T,1)$(Fisher and Zen, 1971)
G'	$\int_{298}^{T}\Delta C_{pfs}dT - T\int_{298}^{T}\Delta C_{pfs}/T\,dT + \Delta V_S(P-1) + N_W G^*_w(T,P)$
r	subscript indicating "of reaction"
s	subscript indicating "due to solids in reactions"

on the functions reported by Krupka et al. (1977, 1979). The heat capacity of end-member anthophyllite was estimated from the properties of the natural mineral measured by Krupka et al. (1979) according to the scheme:

$$C_p(Mg_7Si_8O_{22}(OH)_2) = C_p(Mg_{6.3}Fe_{0.7}Si_8O_{22}(OH)_2) - 0.35C_p(Fe_2SiO_4) + 0.35C_p(Mg_2SiO_4)$$

The heat capacity of fayalite was taken from Robie et al. (1978). The extended Maier–Kelley function obtained was used to calculate heat capacities at 298.15 K and at twenty degree intervals to 700 K. The twenty-two calculated heat capacities were fit by least-squares regression to a three term polynomial to permit extrapolation above 700 K. The heat capacity function for orthorhombic enstatite differs substantially from the one used by Day and Halbach (1979) and was derived by least squares regression on 37 values calculated from the extended Maier–Kelley function reported by Krupka et al. (1979) in the temperature interval 298–1000 K. The heat capacity function for talc was derived by regression on twenty values in the temperature range 298–650 K calculated from the extended function reported by Krupka et al. (1977).

The heat capacity functions for alpha and beta quartz and the enthalpy of the alpha-beta transition (848 K, $\Delta H_{\alpha\beta} = 290$ calories = 1213 J) were taken from Kelley (1960) and are compatible with the compilation of Robie and Waldbaum (1968). These heat capacity functions yield high-temperature heat contents of alpha quartz that are no more than 74 J greater than those preferred by Robie et al. (1978) and Stull and Prophet (JANAF Tables, 1971). However, the heat content of beta quartz at 900 K is 647 J greater than the value preferred by Robie et al. (1978) and Stull and Prophet (1971), most of which (485 J) can be attributed to the higher apparent enthalpy of the alpha–beta transition chosen by Kelley. We have chosen to retain the higher heat contents and heat capacity functions of Kelley (1960) because: (1) a recent unpublished measurement cited by Stull and Prophet (1971) suggests that the JANAF heat content at 968 K may be too low by 314 J and (2) as pointed out by Helgeson et al. (1978, p. 21), integration of the heat capacity functions by assuming that the alpha–beta transition is first order will tend to produce an underestimate of the true heat content of beta quartz. Judging from Figure 3c of Helgeson et al. (1978), the underestimate might be as large as 200–300 J.

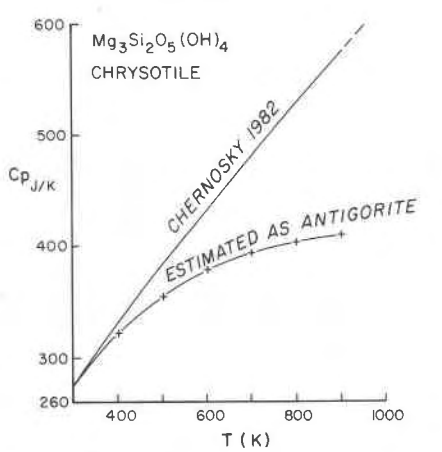

Fig. 3. Comparison of heat capacity functions for chrysotile. The curve from Chernosky was derived by regression analysis of experiments and other calorimetric data (Chernosky, 1982, Column B, Table 4).

The heat capacity function for brucite is a weighted least squares regression on the heat content data reported by King et al. 1975. However, the functions for both antigorite and chrysotile are estimates that require further discussion. Because no high temperature heat capacities are available for chrysotile, we have followed the lead of Robie et al. (1978) and Helgeson et al. (1978) and have assumed that the heat capacity of $Mg_3Si_2O_5(OH)_4$ (antigorite, King et al., 1967) is a good estimate for chrysotile. King et al. (1967) measured the high temperature heat content of antigorite ($Mg_3Si_2O_5(OH)_4$) up to 848 K. Their 11 data were fit by weighted least squares regression to a Maier Kelley function:

$$Cp(J/K) = 346.980 + 95.019 \times 10^{-3}T - 95.759 \times 10^{5}T^{-2}$$

which fits the raw data better than the function provided by King et al. (1967). This estimated function for chrysotile differs in a significant way from the heat capacity function derived by Chernosky (1982). Because no direct measurements have been reported by chrysotile, Chernosky (1982) used least squares regression techniques to derive a heat capacity function that would produce good agreement between hydrothermal experiments and available calorimetric data. Figure 3 illustrates a comparison of the two heat capacity functions. The major differences in these functions may help account for some of the discrepancies discussed later in this paper.

The heat capacity of antigorite ($Mg_{48}Si_{34}O_{85}(OH)_4$) was estimated according to the scheme proposed by Helgeson et al. (1978, p. 64, and Table 2) using the function for $Mg_3Si_2O_5(OH)_4$ reported by King et al. (1967):

$$C_p(Mg_{48}Si_{34}O_{85}(OH)_{62} = 16[C_p(Mg_3Si_2O_5(OH)_4)] + 2\,C_p\,(\alpha\text{-quartz}) - C_p\,(\text{structural water}).$$

$$C_p = 5615.83 + 1554.45 \times 10^{-3}T - 1554.75 \times 10^{5}T^{-2}$$

The heat capacity of structural water was taken from Helgeson et al. (1978, Table 2).

Enthalpies and entropies of formation. Enthalpies and entropies of formation can be calculated from dehydration equilibria using only a knowledge of the molar volumes and heat capacities of the solids and the thermodynamic properties of water, as discussed above. It is useful, however, to compare the values permitted by the experiments with independent measurements. Calorimetric determinations of entropy and enthalpy for the solid phases of interest are listed in Table 4. The properties of brucite, periclase, quartz and talc are taken from Robie et al. (1978) and the sources for the other data are listed in the footnotes. The enthalpies of formation from the elements for enstatite and forsterite were calculated from the heats of solution reported by Charlu et al. (1975) using the heat capacities and heats of formation for the oxides in Robie et al. (1978). The enstatite value is based on the mean of three measured samples and the value for forsterite, on the mean of two samples.

Experimental data base

Pressure–temperature brackets have been determined for the eleven mineral reactions listed in Table 2. These eleven reactions involve nine solid phases and water. Because the first seven reactions in Table 2 define two invariant points linked by reaction 7, only three of those reactions are independent. The sources of the experimental data and the

Table 4. Calorimetrically determined enthalpies and entropies of minerals in the system magnesia–silica–water

PHASE	$S°(298,1)$ (J/K)	$\Delta S°_f(298,1)$[1] (J/K)	$\Delta H°_f(298,1)$ (J)
Anthophyllite	537.0[2] ± 0.5	-2434.72 ± 0.79	-12083059[4] ± 4044
Antigorite	3604.18[8] ± 13.41	-17733.60 ± 13.93	-- --
Brucite	63.18[3] ± 0.065	-305.33 ± 0.095	-924540[3] ± 220
Chrysotile	221.33[7] ± 0.84	-1098.865 ± 0.87	-4361660[3] ± 1740
Enstatite	66.3[2] ± 0.17	-292.915 ± 0.19	-1551237[5] ± 881
Forsterite	94.11[3] ± 0.05	-400.36 ± 0.15	-2173944[6] ± 678
Periclase	26.94[3] ± 0.085	-108.315 ± 0.11	-601490[3] ± 145
α Quartz	41.46[3] ± 0.10	-182.50 ± 0.11	-910700[3] ± 500
Talc	260.83[3] ± 0.32	-1274.03 ± 0.42	-5915900[3] ± 2150

1 Calculated using entropies of the elements reported by Robie et al. (1978).
2 All uncertainties are one standard deviation.
3 Robinson et al. (1982).
4 Robie et al. (1982).
5 Estimate reported by Day and Halbach (1979) based on measurements of Weeks (1956).
6 Calculated as described in text from Charlu et al. (1975).
7 Calculated as described in text from Charlu et al. (1975). An alternative value from Robie et al. (1978) is -2170370 ± 662.
8 King et al. (1967).
Estimated for $Mg_{48}Si_{34}O_{85}(OH)_{62}$ using the entropy reported for antigorite by King et al. (1967) and the estimation scheme advocated by Helgeson et al. (1978).

equations that describe the linear dependence are listed in Table 2.

For the purposes of thermodynamic analysis, we chose to expand all reported experimental temperatures away from the equilibrium curves by five degrees Celsius or the reported temperature uncertainty, whichever is larger. This procedure provides a better estimate of absolute limits on the location of equilibrium curves and offers a better opportunity for obtaining agreement among diverse sets of data gathered in different laboratories by different methods. Except for experiments on the water-conservative reaction number seven, we did not expand pressure measurements in a similar way for two reasons. First, the effect of pressure on the dehydration equilibria and enthalpies and entropies derived from them is small compared to the effect of temperature. Second, many of the reactions considered undergo a change in slope (dP/dT) with increasing pressure so that the direction in which the pressure measurements should be expanded away from the equilibrium becomes ambiguous and a function of the unknown location of the reversal in slope.

We restricted our analysis of anthophyllite-bearing equilibria to the data reported by Chernosky et al. (1985) so that we considered, as nearly as possible, only synthetic phases produced by similar procedures. Chernosky et al. (1985) show a detailed comparison between our results and experiments reported by, among others, Greenwood (1963), Skippen (1971), and Hemley et al. (1977). In general, their work agrees well with our experiments and thermodynamic calculations. Day and Halbach (1979) discussed the difficulties involved in making detailed comparisons among earlier experiments by Chernosky and co-workers and the data of Greenwood (1963) and Hemley et al. (1977). In particular, no feasible solutions were permitted by the combined Chernosky-Greenwood data and Hemley et al. (1977) reported data only at one pressure. Consequently, no attempt was made to incorporate their results in this analysis, despite the overall agreement.

Experiments on reactions one through seven, involving the minerals A, E, F, Q, and T have been summarized by Chernosky et al. (1985, Table 1). Many of the experiments they report resulted in the appearance of phases that are neither reactants nor products of the reaction being studied. In some cases, the appearance of such phases can be rationalized and the experiment may represent a valid reversal. However, in order to take the most conservative approach to the thermodynamic analysis of the data (Chernosky et al., 1985, Table 1), we ignored all experiments containing extraneous phases, all experiments that were clearly redundant based on preliminary inspection, and ambiguous experiments on reaction seven in which reactant and product phases appeared to change in the same direction. In addition, we did not include experiments above ten kilobars for reaction one because the algorithm of Holloway et al. (1971) for the properties of H_2O is limited to lower pressures. All experiments on reactions one through seven that were included in the preliminary thermodynamic calculations are clearly marked in Table 1 of Chernosky et al. (1985).

Experimental data for serpentine-bearing equilibria, reactions eight, nine, and ten, were taken from Chernosky (1982), Johannes (1968) and Evans et al. (1976) respectively. The reader is referred to these papers for discussion of earlier experiments with which the data used here might be compared. Temperature brackets were expanded and experiments at pressures higher than ten kilobars were omitted as previously noted. Two experiments on reaction eight (no. 287t and 215t; Chernosky, 1982) were omitted because talc was not found in the run products. All other experiments that were not obviously redundant were included in the preliminary analysis.

Experimental data for reaction eleven were taken from Schramke et al. (1982) and Barnes and Ernst (1963). Temperature brackets were expanded as already discussed. One bracket reported by Franz (1982) was considered but not used on the grounds that it violates a high temperature reversal by Barnes and Ernst and that it would require a major error in the ΔH_r calculated from the calorimetric data in Table 4. The experiments of Schramke et al. (1982) are internally consistent but the data of Barnes and Ernst (1963) were more difficult to interpret. We did not use the data determined by the "P–T quench" method (Table 1, Barnes and Ernst, 1963) because brucite grew during the early part of the experiments and tended to persist metastably. The most conservative treatment of the remaining

data in Tables 1 and 2 (Barnes and Ernst, 1963) is to accept only the high temperature experiments in which periclase was produced at the expense of brucite. In fact, we found that no feasible thermodynamic solutions existed for reaction eleven if the other experiments were included in the analysis. Consequently, our preliminary analysis of reaction eleven included the data from Schramke et al. (1982) and the high temperature experiments from Barnes and Ernst (1963).

Preliminary thermodynamic analysis

Using the heat capacities and molar volumes listed in Table 1, we expressed each experiment on the eleven reactions considered as a constraint on the enthalpy and entropy of reaction similar to equations (2) and (3). Not all experiments provide equally useful limits on the thermodynamic parameters and such redundant experiments are not considered in subsequent calculations. For example, eleven experiments on reaction 1 were considered and only four provide boundary constraints on the thermodynamic parameters. The relationships among the redundant and boundary constraints are illustrated in Figure 4. For the sake of clarity, only boundary constraints are listed in Table 5 and illustrated in subsequent figures.

Our preliminary treatment of the experimental data shows that the experimental data for each of the eleven reactions determined are internally consistent. That is, the experimental pressure–temperature brackets, heat capacities, molar volumes and Gibbs energy of water define feasible solution spaces similar to that in Figure 4. The feasible solution spaces are defined by and can be constructed directly from the boundary constraints listed in Table 5. In practice, for ease in plotting, our computer program lists the vertices of the feasible polygon in addition to the boundary constraints.

Figures 4, 5, and 6 demonstrate that the experimental data are compatible, broadly speaking, with ΔH°_{fs} and ΔS°_{fs} calculated from the data in Table 4. We consider the data to be "broadly compatible" if the calorimetrically determined enthalpy and entropy in question lie within the ranges permitted by the experiments, although they may not define a coordinate in the feasible solution space. Note that the error bars illustrated in the figures are $\pm$*one* standard deviation.

No significant inconsistencies appear for reactions TEQW, TFEW, AnFTW, CBFW, and BPW (Figs. 4 and 5). All the anthophyllite-bearing reactions (Fig. 6), however, display systematic discrepancies between calorimetric and calculated enthalpies. The discrepancy ranges from 25–40 kJ per gram-formula unit of anthophyllite and a systematic error in the calorimetric enthalpy of about +34 kJ ($\sim$0.3% of ΔH°_f (A)) would eliminate most of the observed difference. In view of the large and estimated corrections made for impurities in the analyzed anthophyllite (~ -50 kJ, Weeks, 1956; Day and Halbach, 1979), we suggest that the hydrothermal experiments may provide a better estimate of the enthalpy of formation.

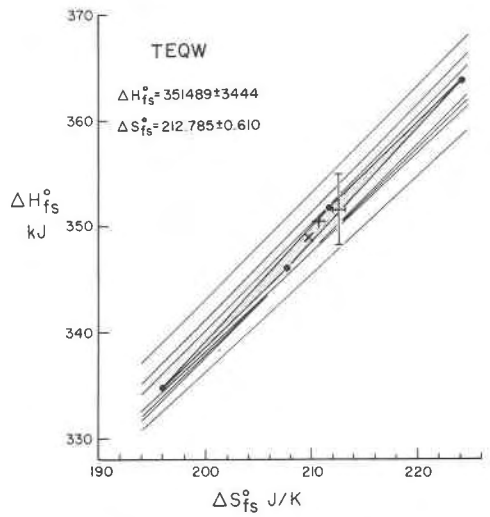

Fig. 4. Feasible solutions of ΔH°_{fs} and ΔS°_{fs} for reaction no. 1: TEQW. The combinations of ΔH°_{fs} and ΔS°_{fs} lying in the shaded region satisfy all experimental brackets, the thermodynamic properties of water and the heat capacity and molar volume data in Table 2. Filled circles are the vertices of the feasible solution space. Lines outside the feasible solution spaces are redundant constraints provided by the experiments indicated in Table 1 of Chernosky et al. (1984). Error bars show the $\pm$ one sigma limits for the ΔH°_{fs} and ΔS°_{fs} calculated from the data in Table 4. The bold (+) and (×) represent the "minimum deviation" data from Table 6 and the "midpoint" from Table 7.

The entropies of the anthophyllite-bearing reactions might also be displaced (Fig. 6) in a way that suggests the calorimetric entropy of anthophyllite is too small. However, increasing the entropy of anthophyllite would increase the disagreement for reaction AFEW (Fig. 6a). In addition, the magnitude of the discrepancies (up to 30 sigma in ΔS°_{fs}) is too large, in our view, to argue that the calorimetric entropy of anthophyllite is the *principal* source of the error. We suggest that most of the error lies in calorimetric enthalpy of anthophyllite, but, as discussed later, some error in the entropy may also be important. Clearly, other sources might also contribute to the discrepancies; for example: (1) disorder in the synthetic anthophyllite, (2) inappropriate extrapolation of the anthophyllite heat capacity function to high temperature, (3) undetected error in the experimental brackets.

Our preliminary analysis suggests that there is a major inconsistency between the experimental and calorimetric data for reaction 8 (CFTW). Figure 7 shows two feasible solution spaces and the values of ΔH°_{fs} and ΔS°_{fs} from Table 4. The shaded part of the diagram is the feasible solution space defined by all the experiments listed in Table 5. If experiment no. 55m (Table 5; Chernosky, 1982, Table 1) is removed, the feasible solution space expands to permit values that are "broadly compatible" with the available

Table 5. Constraints on thermodynamic properties of reactions and minerals. GE and LE mean "greater than or equal to" and "less than or equal to" respectively.

No.	Experimental P,T nominal bars	°C	expanded °C	Constraint on enthalpy and entropy of solids in the reaction T(K)	G'(J)
			R1: T = 3E + Q + W		
35	500	672	677	-1 ΔH(1) + 950.15 ΔS(1) GE	-150394.066
58	1000	700	694	-1 ΔH(1) + 967.15 ΔS(1) LE	-145060.665
54	10000	790	785	-1 ΔH(1) + 1058.15 ΔS(1) LE	-126165.320
56	10000	800	805	-1 ΔH(1) + 1078.15 ΔS(1) GE	-123295.955
			R2: T + F = 5E + W		
16	500	621	626	-1 ΔH(2) + 899.15 Δ S(2) GE	-157451.393
35	1000	652	647	-1 ΔH(2) + 920.15 Δ S(2) LE	-152438.995
10	4000	722	727	-1 ΔH(2) + 1000.15 Δ S(2) GE	-139327.062
30	6000	679	674	-1 ΔH(2) + 947.15 Δ S(2) LE	-146261.440
			R3: A + F = 9E + W		
15	500	667	672	-1 ΔH(3) + 945.15 ΔS(3) GE	-157892.405
22	1000	677	672	-1 ΔH(3) + 945.15 ΔS(3) LE	-154968.377
1	3000	695	700	-1 ΔH(3) + 973.15 ΔS(3) GE	-149608.001
18	5000	684	679	-1 ΔH(3) + 952.15 ΔS(3) LE	-152251.967
8	6000	701	707	-1 ΔH(3) + 980.15 ΔS(3) GE	-149145.574
			R4: A = 7E + Q + W		
23	500	687	692	-1 ΔH(4) + 965.15 ΔS(4) GE	-154281.061
13	1500	752	757	-1 ΔH(4) + 1020.15 ΔS(4) LE	-143372.884
31	10000	810	815	-1 ΔH(4) + 1088.15 ΔS(4) GE	-131640.483
			R5: 7T = 3A + 4Q + 4W		
10	500	647	642	-1 ΔH(5) + 915.15 ΔS(5) LE	-601883.244
5	1000	687	692	-1 ΔH(5) + 965.15 ΔS(5) GE	-564227.008
9	1500	701	706	-1 ΔH(5) + 979.15 ΔS(5) GE	-550094.461
21	3000	727	722	-1 ΔH(5) + 995.15 ΔS(5) LE	-530568.547
16	3000	742	747	-1 ΔH(5) + 1020.15 ΔS(5) GE	-516534.326
			R6: 9T + 4F = 5A + 4W		
11	500	597	590	-1 ΔH(6) + 863.15 ΔS(6) LE	-623471.544
12	500	632	637	-1 ΔH(6) + 910.15 ΔS(6) GE	-600815.570
22	1000	626	621	-1 ΔH(6) + 894.15 ΔS(6) LE	-597714.612
21	1000	646	651	-1 ΔH(6) + 924.15 ΔS(6) GE	-581984.731
15	2000	660	665	-1 ΔH(6) + 938.15 ΔS(6) GE	-565634.425
3	3000	666	661	-1 ΔH(6) + 934.15 ΔS(6) LE	-563617.276
18	4000	677	687	-1 ΔH(6) + 955.15 ΔS(6) GE	-548691.654
17	5000	684	689	-1 ΔH(6) + 962.15 ΔS(6) GE	-542607.261
			R7: T + 4E = A		
2	10300	730	725	-1 ΔH(7) + 998.15 ΔS(7) LE	8857.811
4	10500	755	750	-1 ΔH(7) + 1023.15 ΔS(7) LE	9202.723
6	14300	790	787	-1 ΔH(7) + 1058.15 ΔS(7) LE	10751.932

Table 5. (Cont.)

No.	bars	°C	°C	T(K)	G'(J)
			R8: 5C = 6F + T + 9W		
53m	500	427	432	-1 ΔH(8) + 705.15 ΔS(8) GE	-1591278.505
55m	500	409	414	-1 ΔH(8) + 687.15 ΔS(8) GE	-1612814.709
321t	1000	399	392	-1 ΔH(8) + 665.15 ΔS(8) LE	-1634156.106
289t	2000	431	424	-1 ΔH(8) + 697.15 ΔS(8) LE	-1585386.924
54m	5000	496	491	-1 ΔH(8) + 764.15 ΔS(8) LE	-1480688.139
49m	5000	511	517	-1 ΔH(8) + 790.15 ΔS(8) GE	-1445680.213
44m	6500	536	542	-1 ΔH(8) + 815.15 ΔS(8) GE	-1405575.748
43m	6500	508	503	-1 ΔH(8) + 776.15 ΔS(8) LE	-1458761.778
			R9: C + B = 2F + 3W		
8	1000	370	375	-1 ΔH(9) + 648.15 ΔS(9) GE	-551188.057
12	2000	375	370	-1 ΔH(9) + 643.15 ΔS(9) LE	-551041.059
22	5500	410	405	-1 ΔH(9) + 678.15 ΔS(9) LE	-529935.102
26	7000	440	445	-1 ΔH(9) + 718.15 ΔS(9) GE	-509912.302
			R10: An = 18F + 4T + 27W		
55a	2000	480	475	-1 ΔH(10) + 748.15 ΔS(10) LE	-4553992.891
47b	2000	540	545	-1 ΔH(10) + 818.15 ΔS(10) GE	-4284069.125
49b	6000	560	555	-1 ΔH(10) + 828.15 ΔS(10) LE	-4159768.265
48b	6000	590	595	-1 ΔH(10) + 868.15 ΔS(10) GE	-3996843.616
112	10000	615	610	-1 ΔH(10) + 883.15 ΔS(10) LE	-3887545.066
67	10000	630	635	-1 ΔH(10) + 908.15 ΔS(10) GE	-3782986.728
			R11: B = P + W		
S3	8130	806	811	-1 ΔH(11) + 1084.15 ΔS(11) GE	-11001.360
S4	8090	785	780	-1 ΔH(11) + 1053.15 ΔS(11) LE	-115851.561
S13	5130	720	715	-1 ΔH(11) + 988.15 ΔS(11) LE	-128612.874
S17	3950	690	685	-1 ΔH(11) + 958.15 ΔS(11) LE	-134473.178
BE	1010	607	612	-1 ΔH(11) + 885.15 ΔS(11) GEG	-150338.085

Linear dependence of reactions R1 - R7

1 ΔH(5) + 3 ΔH(4) - 7 ΔH(1) = 0	1 ΔS(5) + 3 ΔS(4) - 7Δ S(1) = 0
1 ΔH(7) + 1 ΔH(4) - 1 ΔH(1) = 0	1 ΔS(7) + 1 ΔS(4) - 1Δ S(1) = 0
1 ΔH(2) - 1 ΔH(3) - 1 ΔH(7) = 0	1 ΔS(2) - 1 ΔS(3) - 1Δ S(7) = 0
9 ΔH(2) - 1 ΔH(6) - 5 ΔH(3) = 0	9 ΔS(2) - 1 ΔS(6) - 5Δ S(3) = 0

Definition of seven independent reactions in terms of participating phases

3H(E) + 1H(Q) - 1H(T) - 1 ΔH(1) = 0	3S(E) + 1S(Q) - 1S(T) - 1 ΔS(1) = 0
5H(E) - 1H(F) - 1H(T) - 1 ΔH(2) = 0	5S(E) - 1S(F) - 1S(T) - 1 ΔS(2) = 0
9H(E) - 1H(F) - 1H(A) - 1 ΔH(3) = 0	9S(E) - 1S(F) - 1S(A) - 1 ΔS(3) = 0
6H(F) + 1H(T) - 5H(C) - 1 ΔH(8) = 0	6S(F) + 1S(T) - 5S(C) - 1 ΔS(8) = 0
2H(F) - 1H(B) - 1H(C) - 1 ΔH(9) = 0	2S(F) - 1S(B) - 1S(C) - 1 ΔS(9) = 0
18H(F) + 4H(T) - 1H(An) - 1 ΔH(10) = 0	18S(F) + 4S(T) - 1S(An) - 1 ΔS(10) = 0
1H(P) - 1H(B) - 1 ΔH(11) = 0	1S(P) - 1S(B) - 1 ΔS(11) = 0

calorimetric data and the heat capacity function estimated for antigorite (Table 1, Fig. 3). Chernosky (1982) observed that calorimetric data are "in reasonable agreement" with the experimental results. However, that apparent agreement was obtained by treating the heat capacity of chrysotile as an adjustable parameter and finding a heat capacity function that fits both the experiments and the calorimetric data. That heat capacity function is very different from the function used here and is illustrated in Figure 3. We have no independent reason to eliminate experiment CFTW no. 55m (Table 5). However, there is also no evidence that the entropies of chrysotile, forsterite and talc could be sufficiently wrong to account for the observed inconsistency. Consequently, we have omitted experiment CFTW no. 55m from subsequent calculations.

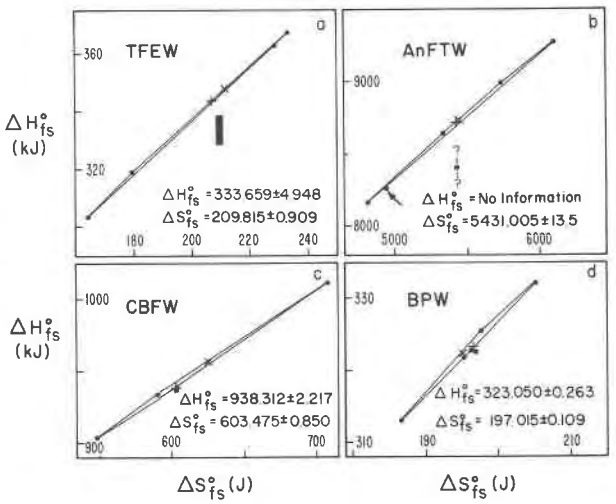

Fig. 5. Relationship between feasible solutions of ΔH°_{fs} and ΔS°_{fs} and the calorimetric data listed in Table 4. a. TFEW b. AnFTW c. CBFW d. BPW. In Figure 5b, the arrow indicates two superimposed vertices. H°_{fs} (An) is unknown so no values of ΔH°_{fs} (AnFTW) are shown. The bold (+) and (×) are the "minimum deviation" data from Table 6 and the "midpoint" from Table 7, respectively. The filled rectangles represent ± one standard deviation of the calorimetric data in Table 4.

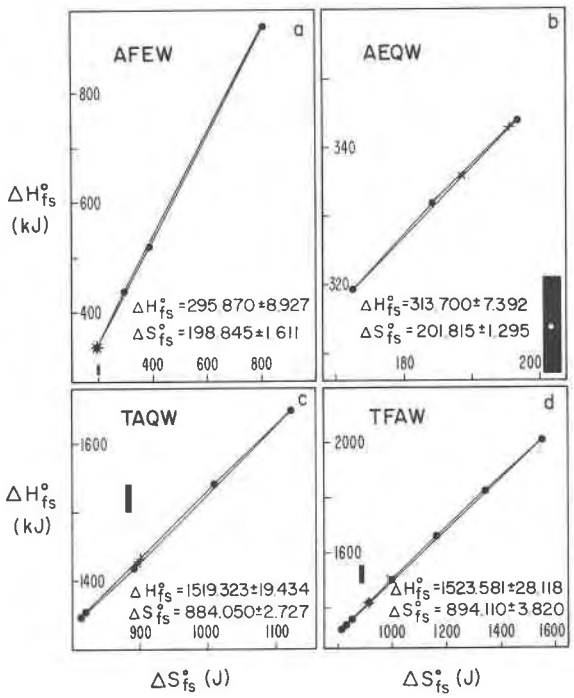

Fig. 6. Relationship between feasible solutions of ΔH°_{fs} and ΔS°_{fs} and the calorimetric data listed in Table 4. a. AFEW b. AEQW c. TAQW d. TFAW. The bold (+) and (×) are the "minimum deviation" data from Table 6 and the "midpoint" from Table 7, respectively. The filled rectangles represent ± one standard deviation of the calorimetric data in Table 4.

The problem of a "best" set of thermodynamic data

Our preliminary analysis makes it clear that the existing calorimetric data and the experimental data are not mutually consistent. Only for reaction TEQW (Fig. 4) do the existing calorimetric data define a point within the feasible solution space. However, all the calorimetric data illustrated in Figures 5 and 7 are within the combined two standard deviations of ΔS°_{fs} and ΔH°_{fs}. Furthermore, if we accept the argument that the enthalpy of anthophyllite is incorrect, no conclusions concerning agreement with the experiments can be drawn from the data in Figure 6. Finally, we note that using the alternate choice for the enthalpy of forsterite (Table 4) does not yield consistently improved agreement for forsterite-bearing reactions.

The preliminary analysis deals with each reaction by itself and neither separates the individual phase properties nor considers all experimental data simultaneously. In this section, we try to identify possible sources of disagreement by examining the "best" agreement with the enthalpies and entropies of each mineral that is permitted by all reactions taken simultaneously. We will argue that in addition to the error in anthophyllite enthalpy discrepancies in the entropy of anthophyllite, and in the enthalpy of enstatite and talc are the most important sources of disagreement between the data sets.

In order to treat all reactions simultaneously and to derive thermodynamic properties of the phases, it is necessary to describe the linear dependence of reactions one through seven (Table 2) and to define each reaction property in terms of the properties of the constituent phases. Table 5 lists the set of constraints that must be solved simultaneously in order to derive properties of the nine solid phases of interest.

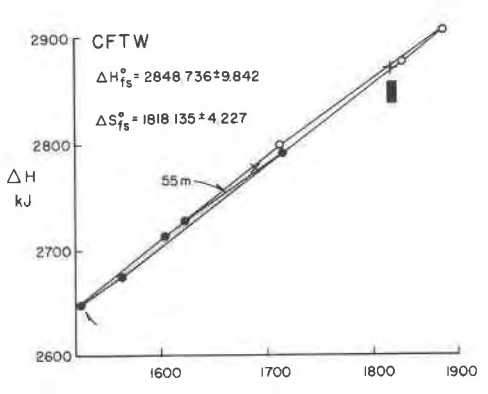

Fig. 7. Two feasible solution spaces for the reaction CFTW. Open circles and the dashed lines outline the expanded feasible solution space that occurs when experiment 55m and its two vertices are removed. The bold (+) and (×) represent the "minimum deviation" from Table 6 and the midpoint from Table 7, respectively. The filled rectangles represent ± one standard deviation of the calorimetric data in Table 4. The arrow indicates two superimposed vertices.

The experimental data (Table 5) and the existing calorimetric data (Table 4) are mutually inconsistent and we would like to know how serious the disagreement is and possible sources of the discrepancies. As a measure of disagreement, we have used the function described in detail by Day and Kumin (1980, p. 272 and appendix):

$$Z = \sum_i \left| \frac{H_i - H_i'}{UH_i'} \right| + \left| \frac{S_i - S_i'}{US_i'} \right|$$

where H_i and S_i are the enthalpy and entropy of phase i that lie within the set of feasible solutions defined by the experiments (Table 5). H_i', S_i', UH_i' and US_i' are the calorimetric values measured by independent means and their associated one sigma uncertainties (Table 4). The function Z is a measure of the distance between calculated and measured values expressed in units of standard deviations.

We have used linear programming methods to find the set of enthalpies and entropies that minimizes Z subject to the constraints listed in Table 5. The choice of derived enthalpies and entropies that is consistent with the experiments and that minimizes the total deviations from the calorimetric data in Table 4 is listed in Table 6 in the column headed "Minimum Deviation". Z was calculated as the sum over all entropies and enthalpies except the enthalpies of anthophyllite and antigorite for which no reliable values are available.

The agreement between derived thermochemical values in Table 6 and the measured values in Table 4 is good, except for the enthalpy of talc and enstatite and the entropy of anthophyllite and, perhaps, enstatite. The derived enthalpy of formation of talc is eight standard deviations more positive than the measured value reported by Robie et al. (1978). The derived enthalpy of enstatite is six standard deviations more positive than the value measured by Charlu et al. (1975) but agrees with the enthalpy of *clino*enstatite within the uncertainty reported by Robie et al. (1978). The derived entropy of anthophyllite is four and one-half standard deviations more positive than the value reported by Robinson et al. (1982) based on unpublished measurements by Krupka.

It is worthwhile to clarify that the perfect agreement of the calculations with many of the calorimetric data in Table 4 does not indicate that the result has been forced in any way to fit the calorimetric results. Not surprisingly, the total deviation simply reaches a minimum when many of the results are in perfect agreement with Table 4. Likewise, the agreement cannot be improved by "taking into account the errors" in the calorimetric data. Such uncertainties already appear in the objective function (Z) and the discrepancies are expressed in Table 6 as the number of standard deviations by which the calculated and calorimetric data differ.

The excellent agreement of most other derived parameters and the very large discrepancies in the enthalpy of talc and enstatite suggest that the enthalpies of formation of these minerals should be redetermined. The source of the apparent discrepancy in the entropy of anthophyllite is not clear. There may be entropy of disorder in the anthophyllite used in the hydrothermal experiments or undetected zero point entropy in the sample used for calorimetry. In addition, the heat capacity function of anthophyllite used in this study (Table 1) is an estimated function based on measurements up to 700 K of natural, impure material (Krupka et al., 1979). The results of our calculations are sensitive to the manner in which the measured heat capacities are corrected for impurities and to the way in which heat capacity is extrapolated to higher temperatures. Consequently, it is possible that the experimentally derived and measured entropies need not disagree.

Table 6. Enthalpies and entropies of formation from the elements from within the feasible solution space*

	Minimum Deviation		Minimax Deviation	
	$-\Delta H_f^\circ$(J)	$-\Delta S_f^\circ$(J/K)	$-\Delta H_f^\circ$(J/K)	$-\Delta S_f^\circ$(J/K)
Antigorite	71435107	17733.000	71482383	17685.153
	—	(0)	—	(3.48)
Anthophyllite	12072854	2431.163	12093535	2432.367
	—	(4.50)	—	(2.98)
Brucite	924828	305.330	924086	305.004
	(1.31)	(0)	(2.06)	(3.43)
Chrysotile	4362379	1098.865	4366156	1095.877
	(0.41)	(0)	(2.58)	(3.43)
Enstatite	1545654	293.342	1548211	293.419
	(6.34)	(2.25)	(3.43)	(2.65)
Forsterite	2173944	400.360	2176273	399.845
	(0)	(0)	(3.44)	(3.43)
Periclase	601490	108.315	601489	108.693
	(0)	(0)	(0.00)	(3.44)
Quartz	910700	182.500	912417	182.122
	(0)	(0)	(3.43)	(3.44)
Talc	5898217	1274.030	5909181	1275.473
	(8.22)	(0)	(3.13)	(3.44)

* Numbers in parentheses represent the number of standard deviations in the measured value by which the calculated value differs from the calorimetric values in Table 4.

We have chosen the coordinate that minimizes the total deviations from measured calorimetric data as our "best" set of thermodynamic data. One can argue that another choice of feasible solutions would require less extreme discrepancies for the enthalpies talc and enstatite. Any such solution, however, must have a larger total deviation. In order to evaluate other such solutions, we have used another objective criterion that we call the "minimax." Using this criterion, we find the coordinate at which the *largest* deviation from a calorimetric value is a minimum. This criterion has the effect of lowering the deviations for talc and enstatite but raising the total deviations and the deviations for most other minerals. The meaning of this criterion is demonstrated most simply by inspecting the list of parameters that defines the minimum total deviation from calorimetric values (Table 6). The enthalpy of talc is the parameter with the largest deviation (8.22 σ) in that list and we inquire whether it is possible to choose a solution that does not require such an extreme discrepancy. The answer

is yes. However, because the solution already lies at the coordinate defining the minimum total deviation, the new solution necessarily requires that the deviation of other parameters and the total deviation must increase. For example, less "error" might be assigned to the enthalpies of talc and enstatite but more "error" must then be assigned to other parameters. The "minimax" criterion is designed to search for a list of parameters such that the largest deviation in the list is as small as possible, subject to the experimental constraints in Table 5.

For the data treated here, the largest deviation from the calorimetric data can be no smaller than 3.44 standard deviations. The data set having this property is listed in Table 6 under the heading, "minimax deviation," and requires significant error in the properties of most phases. Consequently, we prefer the "minimum deviation" data as our "best" set of derived thermochemical parameters.

The problem of a "best" phase diagram

Day and Halbach (1979) analyzed experiments on reactions involving anthophyllite, enstatite, forsterite, quartz, talc, and H_2O and showed that several markedly different topologies of thermodynamically consistent phase diagrams were compatible with the data available. Our new experimental data (Chernosky et al., 1985) now permit only one topology for the stable equilibria among these phases (Fig. 8).

A "best" set of thermochemical data such as the "minimum deviation" data in Table 6 does not necessarily lead to a "best" phase diagram for several reasons. First, neither the "minimum deviation" nor the "minimax" data sets in Table 6 necessarily lies at the maximum of the probability function defined by the standard deviations associated with the calorimetric measurements. Second, the definition of "best" set of thermochemical data implied by accepting the "minimum deviation" measure of goodness of fit is based on agreement with a calorimetric data set that we now suggest may contain important systematic errors. Third, when calorimetric data lie outside the feasible solution defined by the experiments, the "minimum deviation" criterion produces an optimum solution that lies on the *boundary* of the feasible solution space (cf. Day and Kumin, 1980, appendix 2). This result, therefore, requires that at least one calculated equilibrium curve must pass through a limiting experiment rather than between the limiting brackets. Finally, the experiments themselves suggest that a "best" phase diagram should contain equilibrium curves that pass *between* limiting experiments, implying thermochemical parameters that define a coordinate inside rather than on the boundary of the feasible solution space.

The phase diagram illustrated in Figure 8 was calculated from values of the enthalpy and entropy of reaction (ΔH°_{fs}, ΔS°_{fs}, see Table 7) at a "midpoint" of the feasible solution space defined by the constraints listed in Table 5. The "midpoint" was found by the linear programming process outlined by Day and Halbach (1979, p. 819) and is not a unique definition of the "center" of the hyperdimensional feasible solution space. It is, however, a thermodynamically consistent data set that yields calculated reactions that pass between all analyzed experimental brackets.

The reaction properties listed in Table 7 can be inverted to find the enthalpy and entropy of the participating phases only if additional thermodynamic information is assumed because there are only seven independent reactions among the nine minerals of interest. It was possible to find properties of the minerals in the earlier computations (Table 6) because the data H'_i and S'_i, (from Table 4) represented the additional independent information necessary for solving the problem. Thus, we have not presented thermodynamic properties of minerals corresponding to the reaction data in Table 7.

In order to evaluate the range of permissible phase diagrams, we determined ten internally consistent thermodynamic data sets from extreme points of the feasible solution space as outlined by Day and Halbach (1979). Phase diagrams calculated from each of these data sets have the same topology as Figure 8 but the temperatures and pressures of the invariant points [Q] and [F] vary as shown. The [Q] invariant point lies at 7.7 ± 0.5 kbar at about

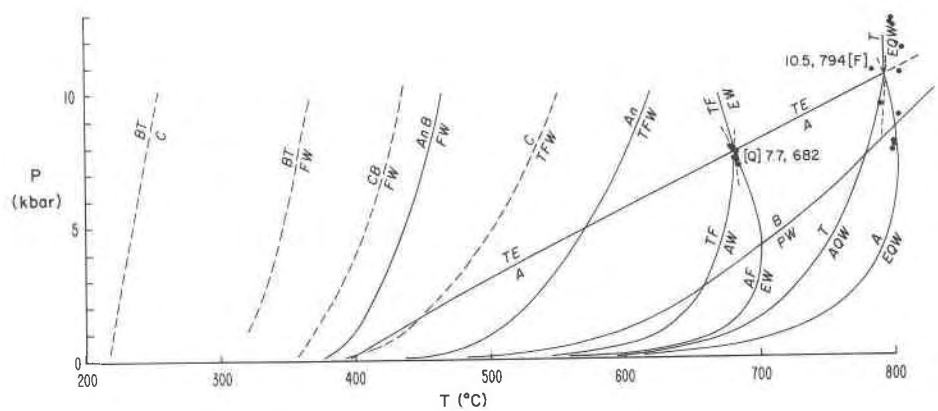

Fig. 8. Phase diagram calculated using the "midpoint" data in Table 7. Filled circles represent the range of permissible locations for the invariant points [Q] and [F] calculated from some extreme points of the feasible solution space defined by Table 5.

Table 7. Enthalpies and entropies at the midpoint of the feasible solution space

Reaction	ΔH°_{fs} (J)	ΔS°_{fs} (J/K)
1. (TEQW)	347118.362	208.269
2. (TFEW)	348431.622	212.470
3. (AFEW)	337744.574	193.355
4. (AEQW)	336431.314	189.154
5. (TAQW)	1420534.592	890.421
6. (TFAW)	1447161.728	945.455
7. (TEA)	10687.048	19.115
8. (CFTW)	2777575.603	1691.393
9. (CBFW)	957046.009	627.974
10. (AnFTW)	8717128.235	5452.882
11. (BPW)	322500.206	195.648

682°C and the [F] invariant point occurs at 10.5 ± 3 kbar at about 794°. We conclude from this exercise that Figure 8 represents the best available estimate of the phase diagram governing the P–T stability of anthophyllite. Phase diagrams calculated from the data in Table 6 are very similar to Figure 8 and must have invariant points within the range illustrated.

No similar conclusion can be stated for the equilibria involving antigorite and chrysotile. Three independent reactions involving serpentine minerals have been determined experimentally (Table 2) and the seven other equilibria considered by Evans et al. (1976) can be calculated from the enthalpies and entropies presented in Tables 6 and 7. Some of these are also illustrated in Figure 8. The seven equilibria calculated from linear combinations of the three experimentally determined reactions are not well constrained. The P–T placement and even direction of these reactions vary widely within the range of permissible thermodynamic parameters and the topology of the serpentine equilibria, therefore, is not determined uniquely by the experimental data presently available.

The serpentine equilibria in Figure 8 are substantially the same as those deduced by Evans et al. (1976). However, the "midpoint" data (Table 7) require that the reaction C = An + F + W lies below 250°C at 1000 bars and chrysotile is therefore metastable above that temperature. The "least deviation" data set in Table 6 requires that chrysotile be metastable with respect to An + B above 25 degrees Celsius at all pressures. It is useful to restate, however, that any conclusion about the metastability of chrysotile is extremely sensitive to choices of enthalpy and entropy from within the range of permissible values.

Conclusions

Our analysis shows that the phase diagram topology first advocated by Greenwood (1963) (Figs. 1a and 8) is the only topology consistent with the experimental data presented by Chernosky et al. (1985) and the mineral properties listed in Table 1. The wide range of permissible phase diagrams illustrated by Day and Halbach (1979) can now be ruled out but some uncertainty remains in the location of invariant points [Q] and [F] (see Fig. 8).

The serpentine equilibria illustrated in Figure 8 must be treated with caution. The hydrothermal experiments considered here (Table 5) and the data in Table 1 are not sufficient to constrain the serpentine equilibria in a meaningful way because so few of the reactions have been determined experimentally. The equilibria in Figure 8 and the data in Tables 6 and 7 are, however, thermodynamically consistent with the anthophyllite equilibria.

Our "best" set of thermodynamic parameters, internally consistent with the phase equilibrium data is listed in Table 6. It includes new values for the enthalpy of formation from the elements (298 K, 1 bar) of antigorite and anthophyllite: −71435 kJ and −12073 kJ respectively.

The combined experimental and thermodynamic approach adopted here and in our companion paper (Chernosky et al., 1984) has raised several issues that deserve further investigation. First, our thermodynamic analysis assumes that the molar volumes, and heat capacities of the minerals are well known and that the properties of water are given exactly by Holloway et al. (1971) and Burnham et al. (1969). Thus, the permissible range of phase diagrams, enthalpies and entropies that we found includes only that variation attributable to the width of the experimental brackets. A second generation of studies might also consider the uncertainty not only in molar volumes, but also in heat capacities and the properties of water.

The thermodynamic analysis of mineral equilibria commonly requires a knowledge of the heat capacity of hydrous minerals significantly above the temperatures at which it is possible to gather useful data. Carefully substantiated models are required that will permit reliable extrapolations of heat capacity to high temperatures. We found also that our analysis of anthophyllite-bearing equilibria was sensitive to the way in which the measured heat capacity of iron-bearing anthophyllite was corrected for the effects of solid solution. Better models for the heat capacity of solid solutions would permit more reliable corrections.

Our analysis suggests possible discrepancies in thermodynamic parameters that might be resolved by further calorimetric determinations. Our "best" set of calculated enthalpies of formation suggests major discrepancies in the value for talc (Table 6). Our value also differs markedly from the one reported by Robinson et al. (1982, $H^\circ_f = -6200218$ J). The other serious discrepancy lies in the enthalpy of formation of enstatite. The value in Table 6 is markedly different from the value determined by Charlu et al. (1975) (cf. Table 4) but is curiously similar to the value reported for *clino* enstatite (Robie et al., 1978, $H^\circ_f = -1548$ kJ). Clearly, the nature of the clinoenstatite–enstatite transition remains a major unsolved problem that will continue to interfere with the careful evaluation of experimental and thermodynamic data.

Finally, it appears to us that further experimental work in this system is unlikely to be rewarding *unless* truly superior starting materials are available that are fully documented, both physically and calorimetrically. This need is

especially critical for talc, anthophyllite, and the serpentines. The most productive approach to further refinement of the anthophyllite-bearing equilibria would be to reverse the reaction T + E = A very tightly at about 675°C.

Acknowledgments

This work has been supported by the National Science Foundation (EAR-77-22775) (Day), EAR-74-13393 and EAR-79-04092 (Chernosky), and EAR-78-24062 (Kumin). We are grateful for the constructive reviews of R. Berman, M. Engi, J. Haas, and J. Rice who, of course, are not responsible for the views expressed here.

References

Burnham, C. W., Holloway, J. R., and Davis, N. F. (1969) Thermodynamic properties of water to 1000°C and 10,000 bars. Geological Society of America Special Paper 32.

Charlu, T. V., Newton, R. C., and Kleppa, O. J. (1975) Enthalpies of formation at 970 K of compounds in the system MgO–Al_2O_3–SiO_2 from high temperature solution calorimetry. Geochimica et Cosmochimica Acta, 39, 1487–1497.

Chatterjee, N. D. (1970) Synthesis and upper stability of paragonite. Contributions to Mineralogy and Petrology, 27, 244–257.

Chatterjee, N. D. (1977) Thermodynamics of dehydration equilibria. In D. G. Fraser, Ed. Thermodynamics in Geology, p. 137–159. D. Reidel, Dordrecht, Holland.

Chernosky, J. V., Jr. (1976) The stability of anthophyllite—a reevaluation based on new experimental data. American Mineralogist, 61, 1145–1155.

Chernosky, J. V., Jr. (1982) The stability of clinochrysotile. Canadian Mineralogist, 20, 19–27.

Chernosky, J. V., Jr. and Knapp, L. A. (1977) The stability of anthophyllite plus quartz. Geological Society of America Abstracts with Programs, 9, 927.

Chernosky, J. V., Jr., Day, H. W., and Caruso, L. J. (1985) Equilibria in the System MgO–SiO_2–H_2O: Experimental determination of the stability of Mg-Anthophyllite. American Mineralogist, 70, 223–236.

Day, H. W. and Halbach, H. (1979) The stability field of Anthophyllite: the effect of experimental uncertainty on permissible phase diagram topologies. American Mineralogist, 64, 809–823.

Day, H. W. and Kumin, H. J. (1980) Thermodynamic analysis of the aluminum silicate triple point. American Journal of Science, 280, 265–287.

Delaney, J. M. and Helgeson, H. C. (1978) Calculation of the thermodynamic consequences of dehydration in subducting oceanic crust to 100 kb and >800°. American Journal of Science, 278, 638–686.

Evans, B. W., Johannes, W., Oterdoom, H., and Trommsdorf, V. (1976) Stability of chrysotile and antigorite in the serpentinite multisystem. Schweizerische Mineralogische und Petrographisch Mitteilungen, 54, 79–93.

Fisher, J. A. and Zen, E-an (1971) Thermochemical calculations from hydrothermal phase equilibrium data and the free energy of H_2O. American Journal of Science, 270, 297–314.

Franz, G., 1982, The brucite–periclase equilibrium at reduced H_2O activities: Some information about the system H_2O–NaCl. American Journal of Science, 282, 1325–1339.

Gordon, T. M. (1973) Determination of internally consistent thermodynamic data from phase equilibrium experiments. Journal of Geology, 81, 199–208.

Greenwood, H. J. (1963) The synthesis and stability of anthophyllite. Journal of Petrology, 4, 317–351.

Hemley, J. J., Montoya, J. W., Shaw, D. R., and Luce, R. W. (1977) Mineral equilibria in the MgO–SiO_2–H_2O system: II Talc–antigorite–forsterite–anthophyllite–enstatite stability relations and some geologic implications in the system. American Journal of Science, 277, 353–383.

Holloway, J. R., Eggler, D. H., and Davis, N. F. (1971) Analytical expression for calculating the fugacity and free energy of H_2O to 10,000 bars and 1,300°C. Geological Society of America Bulletin, 82, 2639–2642.

Johannes, W. (1968) Experimental investigation of the reaction forsterite + H_2O ↔ serpentine + brucite. Contributions to Mineralogy and Petrology, 19, 309–315.

Kelley, K. K. (1960) Contributions to the data on theoretical metallurgy XIII. High temperature heat content heat capacity and entropy data for the elements and inorganic compounds. U. S. Bureau of Mines Bulletin 584.

King, E. G., Barany, R., Weller, W. W., and Pankratz, L. B. (1967) Thermodynamic properties of forsterite and serpentine. U. S. Bureau of Mines Report of Investigations 6962.

Krupka, K. M., Kerrick, D. M., and Robie, R. A. (1977) High temperature heat capacities of dolomite, talc and tremolite and implications to equilibrium in the siliceous dolomite system. Geological Society of America Abstracts with Programs, 9, 1060.

Krupka, K. M., Kerrick, D. M., and Robie, R. A. (1979) Heat capacities of synthetic ortho-enstatite and natural anthophyllite from 5 to 1000 K. EOS, 60, 405.

Orr, R. L. (1953) High temperature heat contents of magnesium orthosilicate and ferrous orthosilicate. American Chemical Society Journal, 75, 528–529.

Robie, R. A., Hemingway, B. S., and J. R. Fisher, J. R. (1978) Thermodynamic properties of minerals and related substances at 298.15 K and 1 bar (10^5 Pascals) Pressure and at Higher temperatures. U. S. Geological Survey Bulletin 1452.

Robie, R. A., Hemingway, B. S., and Takei, H. (1982) Heat capacities and entropies of Mg_2SiO_4, Mn_2SiO_4, and CO_2SiO_4 between 5 and 380 K. American Mineralogist, 67, 470–482.

Robinson, G. R., Jr., Haas, Jr., J. L., Schafer, C. M., and Haselton, Jr., H. T. (1982) Thermodynamic and thermophysical properties of selected phases in the MgO–SiO_2–H_2O–CO_2, CaO–Al_2O_3–SiO_2–H_2O–CO_2 and Fe–FeO–Fe_2O_3–SiO_2 chemical systems, with special emphasis on the properties of basalt and their mineral components. U. S. Geological Survey Open File Report, 83-89.

Schramke, J. A., Kerrick, D. M., and Blencoe, J. G. (1982) Experimental determination of the brucite = periclase + water equilibrium with a new volumetric technique. American Mineralogist, 67, 269–276.

Stemple, I. S. and Brindley, G. W. (1960) A structural study of talc and talc–tremolite relations. Journal of American Ceramic Society, 43, 34–42.

Stephenson, D. A., Sclar, C. B., and Smith, J. V. (1966) Unit cell volumes of synthetic orthoenstatite and low clinoenstatite. Mineralogical Magazine, 35, 838–846.

Stull, D. R. and Prophet, H. (1971) JANAF Thermochemical Tables. National Standard Reference Data Series, U. S. National Bureau of Standards, 37.

Weeks, W. A. (1956) Heats of formation of metamorphic minerals in the system CaO–MgO–SiO_2–H_2O and their petrological significance. Journal of Geology, 64, 456–472.

Zen, E-an (1969) Free energy of formation of pyrophyllite from hydrothermal data: values, discrepancies, and implications. American Mineralogist, 54, 1592–1606.

Manuscript received, November 8, 1983;
accepted for publication, November 19, 1984.